This manuscript updated the recent studies on oxidation mechanism of benzene and phenol, particularly the mechanism of HOMs formation including formation of hydroxybenzenes by successive OH addition, the geminal diol pathways in phenols, and structure rearrangement of bicyclic peroxyl radicals. The mechanism was assessed by the experimental observations under different conditions. The study here identified the dominant role of geminal diol BPRs and their structural rearrangement. The mechanism was also reduced to a small set of 28 species and 30 reactions for greatly reduced computational demanding in 3D modeling while keeping satisfied accuracy. This may be useful in 3D modeling impact on global scale.

The authors thank the reviewer for their feedback and comments on the article. The following paragraphs detail the responses to each comment and the changes made to the manuscript.

Major Comments:

1. Geminal diol BPR: It should be noted that geminal diol from OH addition to ipso-OH-cites often represent a minor channel in reaction of hydroxybenzenes. However, geminal diols contribute higher fractions of SOA in all simulations. Do this suggest SOA formation via Phenol-1OH is higher than that via Phenol-2OH?

Our reply: We fully agree with the reviewer that OH addition to the ipso-OH position is a minor channel. However, the subsequent geminal diol BPR has ring opening (molecular rearrangement) rates on the order of 10s to 1000s s^{-1} (depending on opening side), leading efficiently to HOM. From our previous work (Ojala et al. [accepted]), we found that non-geminal diol BPRs of ortho-, para- and meta-cresol have slow molecular rearrangement rates and are unlikely to contribute to HOM. However, to address the reviewer's comment for phenol specifically, we calculated the molecular rearrangement reaction rates associated with Phenol-2OH BPRs. Only one molecular rearrangement direction was considered, as the other opening direction leads to the formation of energetically unfavorable geminal diol intermediates. Previously it was found that transition state optimization for structures of this type fails, with the optimization reverting to the acid forming one presented here regardless of the used bond constraints. Ojala et al. (2025) The computed molecular rearrangement rate coefficients are slow (3×10^{-3} s^{-1} to 4×10^{-4} s^{-1} , in agreement with previous work for the molecular rearrangement of 2OH-BPRs of cresols Ojala et al. (2025)

Sentences added to the manuscript: **This means that the minor geminal diol BPR pathway can have a disproportionately high contribution to the SOA yield. (line 175)**

Sentences added to the manuscript: **The possibility of HOM formation via molecular rearrangement of BPRs formed from ortho-position OH**

addition was considered. Only one molecular rearrangement direction was considered, as the other opening direction leads to the formation of energetically unfavorable geminal diol intermediates. Previously it was found that transition state optimization for structures of this type fails, with the optimization reverting to the acid forming one presented here regardless of the used bond constraints Ojala et al. (2025). The reaction and associated rate coefficients are presented in figure 1. These were found to be too slow to be atmospherically competitive and thus not implemented into the model. However, we note that the molecular rearrangement transition state in 1 a) suffers from some spin contamination (S^2 value of 0.77), indicating higher uncertainties in the calculated rate coefficient. (line 246)

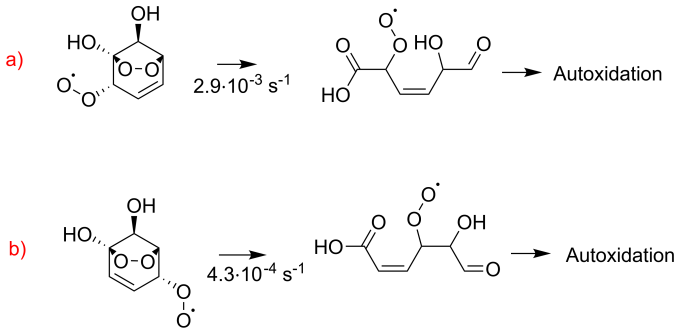

Figure 1: **Molecular rearrangement of BPRs formed from ortho-position OH addition. The molecular rearrangement rate coefficients were found to be too slow to be atmospherically competitive**

2. Line 194: If F12 energies were calculated for the lowest-energy conformers only, what's the basis for MC-TST calculations ?

Our reply: The MC-TST equation includes a Boltzmann weighted contribution of the partition functions of multiple low-lying conformers of the transition state and reactant. For the actual barrier of the reaction, only the lowest-energy conformers of reactant and transition state are used, and consequently only those energies were further refined at the F12 level of theory. This has been shown to be a cost-effective way to calculate rate coefficients, where as calculating the F12 correction for all conformers increases notably the computational cost with diminishing benefits Møller et al. (2016).

Sentences added to the manuscript: **The MC-TST equation includes a Boltzmann weighted contribution of the partition functions of multiple low-lying conformers of the transition state and reactant.**

Additional changes to manuscript: **Further refining at ROHF-ROCCSD(T)-F12a/VDZ-F12 (abbreviated F12) level of theory is done for the lowest energy conformers of all studied molecules, and the IRC endpoints, whereas ωB97 level of theory is used for the relative energies of the conformers. This has been shown to be a cost-effective way to calculate rate coefficients, where as calculating the F12 correction for all conformers increases notably the computational cost with diminishing benefits Møller et al. (2016). CCSD(T) corrections were not performed for H-shift reactions from OH groups, as the F12-level calculations for this reaction class have previously been shown to lead to artifact solutions (Møller et al., 2019).**

3. Line 221-223: "Phenol has only one BPR isomer due to the symmetry of the molecule". This statement is only true for Phenol-1OH adduct, which, as stated above, is the minor channel in reaction of phenol and OH. Instead, Phenol-2OH should lead to two different BPRs as Phenol-2OH-1,3-OOs-4OOa and Phenol-2OH-1,3-OOs-6OOa.

Our reply: The molecular rearrangement of Phenol-2OH was added into the main manuscript (see previous comment), and the line in question was clarified to be about the geminal diol BPRs specifically.
Manuscript changed to read: **Phenol has only one geminal diol BPR isomer due to the symmetry of the molecule**

4. # Figure 4a: The C6H7O8 radical is a carbonyl peroxyl radical, which might have a fast H-atom shift from the -OOH group according to the result from the Demark group.

Our reply: We agree with the reviewer that there is likely a fast H-scrambling pathway between the hydroperoxy acyl peroxy and peroxy peroxoic acid radical forms. This pathway is now added to the Figure 4a of the main manuscript. This pathway doesn't impact the model, as the volatility calculation assumes that the peroxy radicals react with the HO2 to form hydroperoxides, and both C6H7O8 radicals (before and after H-shift from -OOH group) produce identical hydroperoxides. The H-scrambling in question was added to Figure 4a and the text in bold was added to the main text:

The C_1 pathway for phenol yields a $C_6H_7O_6$ peroxy radical that can undergo a 1,6 aldehydic H-shift followed by $_2$ addition to form a $C_6H_7O_8$ peroxy radical (Fig. 4 a). **This can undergo H-scrambling between the hydroperoxy acyl peroxy and peroxy peroxoic acid radical forms, with the latter being thermodynamically more favored (Knap and Jørgensen,**

2017). However, both $C_6H_7O_8$ peroxy radical isomers form identical hydroperoxides following the reaction with HO_2. Since it is the hydroperoxide from that is considered in volatility calculations, the model is unaffected by the peroxy radical isomer in the mechanism.

5. Supplement S2 contains only the gas-phase reactions, while modeling study contains gas-particle partitioning and multiphase chemical processes. I would suppose the authors adopted these processes from SSH-aerosol v2.0 model. What about the 'new' species added in this study?

Our reply: We thank the reviewer for this comment. As mentioned, the reaction mechanism provided in the Supplement contains the gas-phase chemical reactions, whereas the simulations also include the gas–particle partitioning and multiphase processes implemented in the model: in SSH-aerosol v2.0, gas–particle partitioning of organic species is determined using the SOAP thermodynamic module. For each compound provided in the gas-chemistry scheme, the molecular structure provided as a SMILES representation is decomposed into UNIFAC functional groups, while its saturation vapour pressure is estimated using UManSysProp (Topping et al., 2016), following the vapor pressure and boiling point method from Nannoolal et al. (2004) and Nannoolal et al. (2008). With the SMILES structure and the saturation vapour pressure, we calculate the corresponding Henry constant using the thermodynamic module SOAP. The species are subsequently assigned as hydrophilic, hydrophobic, or both, determining whether partitioning into the aqueous phase, organic phase or both phases is considered. No additional particle-phase chemical reactions were introduced for the newly added species, their contribution to SOA formation only results from physical partitioning unto the particle phase. To clarify this point, the tables in Supplementary S2 and S4 have been detailed and now present the P^{sat} values, Henry constants and vaporization enthalpy for the gaseous species considered for SOA formation in the model and simulations.

6. The authors stated "H-abstraction from the aromatic ring" (Line 80), "7%/30% abstraction branching ratio for reactions of benzene and phenols with OH" (Line 343), and "for OH addition and H abstraction in reactions of phenols with OH" (title of Table 2). I would expect all these H-abstractions were for H-abstraction from -OH group of phenol. Direct H-abstraction from aromatic ring is usually ignored under the atmospheric conditions.

Our reply: The reviewer is correct. The following sentence has been modified in the main text to clarify and emphasize the difference between both processes (Line 80).

Manuscript changed to read: **"In addition to the H-abstraction from the hydroxyl group, OH can react with phenols via addition to the aromatic ring"**

7. Mechanism Evaluation as Shown in Figure 5: Mech1 and Mech2 perform obviously better than MCM. In Mech1 and Mech2, adding the overlooked HOMs formation results in new mass balance for SOA mass. The difference in this bar chart simply reflects the different branching ratios in the mechanisms. Agreement of SOA mass with the experimental data may not be able to discriminate Mech1 and Mech2.

Our reply: We thank the reviewer for this important comment. We agree that agreement with total SOA mass alone cannot fully discriminate between Mech1 and Mech2. Nevertheless, Mech2 provides a better representation of the experimental results within the framework considered here, especially when considering the experiments where multihydroxylation is dominant, the overestimation of SOA mass obtained with Mech1 is reduced when the geminal-diol oxidation pathway is included in Mech2. To further discriminate between both mechanisms, we have added Supplementary S10 and S11 which present the functional group composition of SOA obtained using our simulations, and the results of Borrás and Tortajada-Genaro (2012) in terms of composition. The graphs derived from Borrás and Tortajada-Genaro (2012) suggest that the proportion of oxygen-containing species is significant in the particulate phase, including substantial contributions from dicarboxylic compound. Alkyl groups and carbon double bonds account for a smaller fraction of the total SOA mass in most cases, particularly in the H2O2 experiments. These results allow us to distinguish between the two mechanisms as they are more consistent with SOA composition obtained using Mech2. The discussion of Figure 5 has been revised to clarify this point.

Sentences added to the manuscript: **For comparison with experimental observations, Supplement S11 presents the functional-group composition derived from the benzene SOA measurements of Borrás and Tortajada-Genaro (2012). These measurements indicate a substantial contribution of oxygen-containing species to the particulate phase, including dicarboxylic compounds, while alkyl groups and carbon–carbon double bonds generally account for smaller fractions of the SOA mass, particularly in the H2O2 experiments. The higher degree of oxygenation and the presence of dicarboxylic compounds observed experimentally are more consistent with the composition predicted by Mech 2 than with Mech 1, providing additional support for the inclusion of the geminal-diol oxidation pathway.**

8. Line 445: "Stronger photochemical activity and higher OH concentration in summer favor SOA formation via geminal diol pathway". The fractions of different reaction pathways would vary with temperature, and photochemical activity and OH concentration would affect SOA formation via secondary reactions of intermediates. Importance of autoxidation would also vary with temperature and NO/RO2 concentrations. In winter, "reduced photochemical activity" should be "slow intramolecular H shift" in RO2 radicals, therefore self-reactions of RO2

become more important.

Our reply: We thank the reviewer for this comment. In the developed mechanism, the rate coefficients used for the intramolecular H-shift of RO2 radicals are not temperature-dependent, nor are the RO2 + RO2 reactions detailed in the autoxidation scheme. Among the reactions involving RO2 radicals, temperature dependence is considered only for RO2 + NO and RO2 + HO2. Therefore in our simulations, termination pathways of peroxy radicals are influenced by temperature dependent reactions but the seasonal differences in pathway contributions mainly stems from changes in OH and NOx concentrations, associated with seasonal variations in photolysis rates. We have revised the main article to clarify this point.

Manuscript changed to read: **Stronger photochemical activity and higher OH concentration in summer favor SOA formation via OH addition and geminal diol formation.**
In winter, reduced photochemical activity induces lower oxidant levels, resulting in less competition for RO2 self-reactions and intramolecular H-shifts. This leads to a dominant contribution of autoxidation products to SOA mass, even in urban conditions.

9. Reduced Mechanism: Reactions in Supplement S4 do not match the reaction routes in Figure 10.

Our reply: The authors thank the reviewer for this comment. Supplement S4 was supposed to list the reactions in the reduced mechanism but, by mistake, it contained the first reactions of the mechanism Mech2. The table has been corrected in the Supplementary Materials to match the reactions shown in Figure 10.

Minor Comments:

Line 86: "the formation of BPRs through H abstraction and O2 addition". Should it be "through OH addition and O2 addition"?

Our reply: We agree with the reviewer. The sentence has been changed to "lead to the formation of BPRs through OH addition and O2 addition".

Line 87: "RO2 + NO" should be "RO2 + HO2" in order to form alkyl peroxides.

Our reply: We agree with the reviewer. The sentence has been changed to "alkyl peroxides through RO2 + HO2 reactions".

Figure 1: (1) Citation to Fu et al. should be added to figure caption, also proper citation to Figure 2. (2) B-RONO2 and B-ROOH were used in Figure 1, but

T-RONO2 and T-ROOH were used in the text.

Our reply: The difference in terminology between the figure and the text stems from the difference between the article by Fu et al. (2023) dealing with toluene, and the results derived for benzene described in the article. The citation has been added to the caption of Figure 1 and the following sentence has been added to the manuscript to clarify the difference between the T- and B-labeled species.

Sentences added to the manuscript: **Following the nomenclature of Fu et al. (2023) for toluene, species introduced in the benzene oxidation scheme are named BEPOX, B-ROOH, and B-RONO2.**

P1 of Supplement S1: "the correct value" (after Table S1) should be "the corrected value".

Our reply: The wording has been changed from "correct" to "corrected".

Figure 4b: Two structures shown as diradical are incorrect.

Our reply: Changes to manuscript: The structure in Figure 4b was corrected.

Line 380: "C6H603" should be "C6H6O3".

Our reply: The name of the compound has been corrected.

References

Borrás, E. and Tortajada-Genaro, L. A.: Secondary Organic Aerosol Formation from the Photo-Oxidation of Benzene, Atmos. Environ., 47, 154–163, https://doi.org/10.1016/j.atmosenv.2011.11.020, 2012.

Fu, Z., Ma, F., Liu, Y., Yan, C., Huang, D., Chen, J., Elm, J., Li, Y., Ding, A., Pichelstorfer, L., Xie, H.-B., Nie, W., Francisco, J. S., and Zhou, P.: An overlooked oxidation mechanism of toluene: computational predictions and experimental validations, Chem. Sci., 14, 13 050–13 059, https://doi.org/10.1039/D3SC03638C, 2023.

Knap, H. C. and Jørgensen, S.: Rapid Hydrogen Shift Reactions in Acyl Peroxy Radicals, The Journal of Physical Chemistry A, 121, 1470–1479, https://doi.org/10.1021/acs.jpca.6b12787, 2017.

Møller, K. H., Otkjær, R. V., Hyttinen, N., Kurtén, T., and Kjaergaard, H. G.: Cost-Effective Implementation of Multiconformer Transition State Theory for

Peroxy Radical Hydrogen Shift Reactions, J. Phys. Chem. A, 120, 10 072–10 087, https://doi.org/10.1021/acs.jpca.6b09370, pMID: 27992191, 2016.

Møller, K. H., Bates, K. H., and Kjaergaard, H. G.: The Importance of Peroxy Radical Hydrogen-Shift Reactions in Atmospheric Isoprene Oxidation, J. Phys. Chem. A, 123, 920–932, https://doi.org/10.1021/acs.jpca.8b10432, 2019.

Nannoolal, Y., Rarey, J., Ramjugernath, D., and Cordes, W.: Estimation of pure component properties: Part 1. Estimation of the normal boiling point of non-electrolyte organic compounds via group contributions and group interactions, Fluid Phase Equilib., 226, 45–63, https://doi.org/10.1016/j.fluid.2004.09.001, 2004.

Nannoolal, Y., Rarey, J., and Ramjugernath, D.: Estimation of pure component properties: Part 3. Estimation of the vapor pressure of non-electrolyte organic compounds via group contributions and group interactions, Fluid Phase Equilib., 269, 117–133, https://doi.org/10.1016/j.fluid.2008.04.020, 2008.

Ojala, A., Iyer, S., Le Bayon, A., Kumar, A., Vinkvist, N., Savolainen, A., Kervinen, A., Sartelet, K., and Rissanen, M.: Secondary organic aerosol formation from sequential oxidation of toluene and cresols, https://doi.org/10.21203/rs.3.rs-7621262/v1, unpublished, 2025.

Topping, D., Barley, M., Bane, M. K., Higham, N., Aumont, B., Dingle, N., and McFiggans, G.: UManSysProp v1.0: an online and open-source facility for molecular property prediction and atmospheric aerosol calculations, Geosci. Model Dev., 9, 899–914, https://doi.org/10.5194/gmd-9-899-2016, 2016.